Age class structure in SIRD models for the COVID-19 - An analysis of Tennessee data

Age class structure in SIRD models for the COVID-19 – An analysis of Tennessee data

Giuseppe C. Calafiore and Giulia Fracastoro

***Abstract*— The COVID-19 pandemic is bringing disruptive effects on the healthcare system, economy and social life of countries all over the world. Even though the elder portion of the population is the most severely affected by the coronavirus disease, the counter-measures introduced so far by the governments do not take into account age structure, and the restrictions act uniformly on the population irrespectively of age. In this paper, we introduce a SIRD model with age classes for studying the impact on the epidemic evolution of lockdown policies applied heterogeneously on the different age groups of the population. The proposed model is then applied to COVID-19 data from the state of Tennessee. The simulation results suggest that a selective lockdown, while having a lighter socio-economic impact, may bring benefits in terms of reduction of the mortality rate that are comparable to the ones obtained by a uniform lockdown.**

I. Introduction

Governments across the globe are struggling to face the global COVID-19 pandemic, enacting rules aimed at limiting the spread of the contagion and at safeguarding the capacity of the healthcare systems, ultimately protecting the population from the most adverse outcomes of the disease. To date (January 2021) the coronavirus disease has produced a total of about 95 million cases worldwide, and 2 million deaths [1]. The United States have been one of the most severely hit countries, with a total of over 24 million cases and 4 hundred thousand deaths to date [2]. The counter-measures enforced for controlling the contagion have been of diverse intensity in different countries, ranging from bland (e.g., in Sweden) to medium (e.g., USA) and strong (e.g., Italy and China) [3], [4], [5]. In all cases, the control measures included bans of various degree in personal mobility and travel, closures of commercial activities, bars, shops and restaurants, interdiction of gathering in public places such as parks and beaches, closure of schools and, in extreme cases, the shut down of industrial activities. One common aspect of these restrictions, however, was that they acted over the population irrespective of age. This somehow contrasts with the fact that the effects of the coronavirus disease appear to have increasing severity with the age of the infected individuals, the elderly unfortunately accounting for a large portion of the fatal cases [6], [7], [8]. Figure 1, for instance, shows the percent mortality from the coronavirus disease in the USA in function of the age class of the population: the mortality of the elder class of individuals aged 85 or more is 300 times higher than that of individuals in the 25–34 years range. This heterogeneity in the age distribution of mortality has been observed also in other countries, with similar trends [9], [10]. Clearly, in principle, heterogeneity in the mortality distribution can be attributed to (i) the age dependency in susceptibility to the infection and/or to (ii) the age dependency of the severity of the symptoms and outcome of the disease. A recent study [11] on COVID-19 cases in Italy, Japan and Spain, however, indicates that the contribution of age-dependency to susceptibility is not supported by existing data, while the age-dependencies of the mortality rate seems to determine the age distribution in mortality from COVID-19.

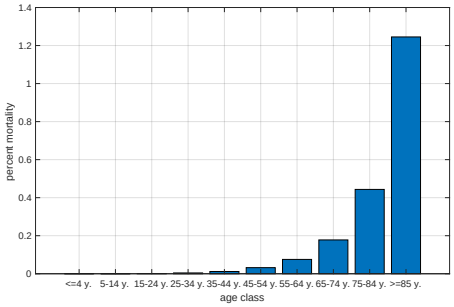

Fig. 1. Mortality of the coronavirus disease in USA per age class. Based on COVID-19 data from `https://data.cdc.gov/NCHS/Provisional-COVID-19-Death-Counts-by-Sex-Age-and-S/9bhg-hcku`, updated Dec. 9, 2020, and on demographics data from `https://www.statista.com/statistics/241488/population-of-the-us-by-sex-and-age`.

The situation in most countries is thus such that on the one hand the part of the population of schooling age and of working age is the most strongly impacted by the governments' restrictions and, on the other hand, the same portion of the population is the least affected by the infection, at least in terms of mortality. The importance of the population age structure in determining the pandemic's progression and impact has been well recognized by researchers, see, e.g., [6]. Indeed, demographic science shows how the effects of the pandemic can be dramatically different in populations with similar sizes but different age structures. Despite this evidence, however, governments have so far neglected age structure in the definition of their policies against the pandemic. Even data on case and fatality disaggregated by age is scarcely available to researchers, and calls for countries to provide this data have been repeatedly made, see, e.g., [6], [12]. Also, in a quite debated and controversial declaration [13], a group of renowned scientists claimed that current lockdown policies are producing devastating effects on short and long-term public health and, recognizing that vulnerability to death from COVID-19 is very different

The authors are with Department of Electronics and Telecommunications, Politecnico di Torino, 10129 Torino, Italy `name.surname@polito.it`

in young-aged subjects than it is in the elder, proposed a "focused protection" approach, whose philosophy would be "to allow those who are at minimal risk of death to live their lives normally to build up immunity to the virus through natural infection, while better protecting those who are at highest risk."

In this paper we explore via an analytical model the effects on the contagion evolution of control policies that act heterogeneously on the different age groups of the population. First, we propose a modified SIRD model with age classes for describing the mean-field time evolution of the number of susceptible, infected, recovered and deceased individuals in each of the considered age groups. Then, we pose this model in a suitable regression form which is amenable to an efficient numerical scheme for the identification of the key model parameters from real observed data. This model is trained on COVID-19 data from the state of Tennessee, covering the period from July 27th to December 16th. This choice was dictated by the fact that, to the best of our efforts, this was the only country for which the required age-class data was publicly available. The considered data period covers the early stages of the contagion [14]. We used the parameters estimated for this model to project forward in time the evolution of the contagion, assuming for this simulation that no further lockdown measures are taken. This simulation constitutes the reference baseline for evaluating the effects of control measures. Control policies are next introduced in the model, in the form of decreasing time profiles of the transmission rate parameters of the age classes. Uniform lockdown policies are simulated by decreasing in the same way the transmission rates of all age classes, while selective lockdown policies are simulated by decreasing only the transmission rates of certain age classes.

The results of these numerical experiments, described in Section V, suggest that a selective lockdown applied only on the older portion of the population can significantly reduce the spread of the epidemic, nearly halving the number of deaths compared to a scenario where no lockdown policies are applied. Moreover, the results show that the effects of a selective lockdown on the mortality rate are similar to the ones obtained with a uniform lockdown, even though the latter one has a much stronger impact on the economy.

II. A MODIFIED SIRD MODEL WITH AGE CLASSES

We consider a geographical region, assumed as isolated from other regions, and within such region we let the population be divided in K non-overlapping age classes. For each class i, $i = 1, \dots, K$, we define the following quantities:

- $S_i(t)$: the number of individuals in the ith class *susceptible* of contracting the infection at day t;
- $I_i(t)$: the number of individuals in the ith class that are alive and *infected* at day t;
- $R_i(t)$: the cumulative number of individuals in the ith class that *recovered* from the disease up to day t;
- $D_i(t)$: the cumulative number of individuals in the ith class that are *deceased* due to the disease, up to day t.

The following assumptions underpin the model we develop: (a) individuals do not change age class as t evolves, that is the age class is assigned at time $t = 0$ and then remains fixed for the time range of our study; (b) the region under consideration is assumed to be isolated from other regions, so that the total population remains constant in size; (c) the recovered subjects are no longer susceptible of infection, at least within the time range of our study; (d) deaths due to other reasons (different from the disease under consideration) are neglected. We let

$$C(t) \doteq S(t) + I(t) + R(t)$$

denote the total number of circulating individuals in the population, being

$$S(t) \doteq \sum_{i=1}^{K} S_i(t), \quad I(t) \doteq \sum_{i=1}^{K} I_i(t), \quad R(t) \doteq \sum_{i=1}^{K} R_i(t).$$

The ratio $S_i(t)/C(t)$ represents the fraction of susceptible individuals of class i in the circulating population. The probability of encountering a susceptible individual of class i can thus be assumed to be proportional to $S_i(t)/C(t)$, with a proportionality factor $c_i(t)$ that represents the level of social activity of individuals in the ith class. An infected individual (of any class) thus has a probability $c_i(t)S_i(t)/C(t)$ of entering into contact with a susceptible individual of class i, and once such contact takes place, there is a probability υ that it results in a contagion, where υ is the probability of infection transmission of the virus. Overall, the average number of new daily contagions in class i generated by *one* infected individual is $\upsilon c_i(t)S_i(t)/C(t)$. Consequently, the average total number of new contagions in class i generated collectively by all the infected individuals during day t is

$$\delta_i(t) \doteq I(t)\beta_i(t)\frac{S_i(t)}{C(t)},$$

where we defined the *transmission rate* parameter for the ith class as $\beta_i(t) \doteq \upsilon c_i(t)$. Further, during day t a fraction $\gamma_i(t)$ of the infected individuals in class i recovers, and a fraction $\nu_i(t)$ of them dies from the disease. The above setup leads to the formulation of the following discrete-time dynamic equations for the evolution of the contagion: for $i = 1, \dots, K$ and $t = 0, 1, \dots$,

$$S_i(t+1) = S_i(t) - \beta_i(t)I(t)\frac{S_i(t)}{C(t)} \tag{1}$$

$$I_i(t+1) = I_i(t) + \beta_i(t)I(t)\frac{S_i(t)}{C(t)} - \gamma_i(t)I_i(t) - \nu_i(t)I_i(t) \tag{2}$$

$$R_i(t+1) = R_i(t) + \gamma_i(t)I_i(t) \tag{3}$$

$$D_i(t+1) = D_i(t) + \nu_i(t)I_i(t). \tag{4}$$

The model is initialized at some conventional $t = 0$ with values $S_i(0) > 0$, $I_i(0) > 0$, $R_i(0) \geq 0$, and $D_i(0) = 0$, for $i = 1, \dots, K$. Notice that it holds for all $i = 1, \dots, K$ that

$$\begin{aligned} &S_i(t+1) + I_i(t+1) + R_i(t+1) + D_i(t+1) \\ &= S_i(t) + I_i(t) + R_i(t) + D_i(t) = N_i, \quad \forall t, \end{aligned}$$

where $N_i = S_i(0) + I_i(0) + R_i(0) + D_i(0)$ is the initial total population for the ith class. The ith class population N_i is assumed to be a fixed fraction α_i of the total population N exposed to the contagion. The fractions α_i, $i = 1, \ldots, K$, are obtained from demographic data. The total exposed population N is in turn assumed to be only a portion of the actual population Pop of the region of interest. Denoting by $\omega \in [0, 1]$ the (unknown) coefficient of proportionality in $N = \omega$Pop, we have that

$$S_i(t)+I_i(t)+R_i(t)+D_i(t) = N_i = \alpha_i N = \alpha_i \omega \text{Pop}, \ \ \forall t \geq 0,$$

where α_i is given, while ω is one of the model parameters to be estimated from the observed data. The last equation is used in the identification phase for obtaining the number of susceptible individuals in the ith class, since this number is not directly measurable otherwise:

$$S_i(t) = \alpha_i \omega \text{Pop} - I_i(t) - R_i(t) - D_i(t). \tag{5}$$

III. Model identification

We first consider a constant-parameter version of the model; the time varying extension is then discussed in Section III-B.

A. Regression model with constant parameters

If $\beta_j(t) = \beta_j$, $\gamma_j(t) = \gamma_j$, and $\nu_j(t) = \nu_j$ for all t and all $j = 1, \ldots, K$, the model (1)–(4) can be rewritten in the following regression form, for $i = 1, \ldots, K$ and $t = 0, 1, \ldots$

$$\boldsymbol{\Delta}_i(t+1) = \boldsymbol{\Phi}_i(t, \omega)\boldsymbol{\theta}, \tag{6}$$

where

$$\boldsymbol{\Phi}_i(t,\omega) \doteq \begin{bmatrix} -\frac{S_i(t)}{C(t)} I(t) \boldsymbol{e}_i^\top & \mathbf{0}_K^\top & \mathbf{0}_K^\top \\ \frac{S_i(t)}{C(t)} I(t) \boldsymbol{e}_i^\top & -I_i(t)\boldsymbol{e}_i^\top & -I_i(t)\boldsymbol{e}_i^\top \\ \mathbf{0}_K^\top & I_i(t)\boldsymbol{e}_i^\top & \mathbf{0}_K^\top \\ \mathbf{0}_K^\top & \mathbf{0}_K^\top & I_i(t)\boldsymbol{e}_i^\top \end{bmatrix},$$

$$\boldsymbol{\theta} \doteq \begin{bmatrix} \boldsymbol{\beta} & \boldsymbol{\gamma} & \boldsymbol{\nu} \end{bmatrix}^\top,$$

$\mathbf{0}_K$ is a vector of zeros of dimension K, $\boldsymbol{e}_i$ is a vector of dimension K with a one in position i and zeros elsewhere, $\boldsymbol{\beta}^\top \doteq [\beta_1 \ \cdots \ \beta_K]$, $\boldsymbol{\gamma}^\top \doteq [\gamma_1 \ \cdots \ \gamma_K]$, $\boldsymbol{\nu}^\top \doteq [\nu_1 \ \cdots \ \nu_K]$, and

$$\boldsymbol{\Delta}_i(t+1) \doteq \begin{bmatrix} S_i(t+1) - S_i(t) \\ I_i(t+1) - I_i(t) \\ R_i(t+1) - R_i(t) \\ D_i(t+1) - D_i(t) \end{bmatrix}.$$

Our objective is to identify the model parameters $\omega \in [0, 1]$ and $\boldsymbol{\theta} \geq 0$ on the basis of observed data. For a given time horizon $T > 0$, the observed data at $t = 0, 1, \ldots, T$, are $I_i(t)$, $R_i(t)$, $D_i(t)$ for each class $i = 1, \ldots, K$. From these data, and for given ω, we construct $S_i(t)$ according to (5). Notice that the transition matrix $\boldsymbol{\Phi}_i(t, \omega)$ depends on ω nonlinearly, through the dependence of $S_i(t)$ on ω.

We next define a quadratic cost with forgetting factor $w \in (0, 1]$

$$f(\omega, \boldsymbol{\theta}) \doteq \frac{1}{T} \sum_{t=0}^{T-1} w^{T-t} \sum_{i=1}^{K} \|\boldsymbol{\Delta}_i(t+1) - W\boldsymbol{\Phi}_i(t, \omega)\boldsymbol{\theta}\|_2^2, \tag{7}$$

where W is a diagonal weight matrix, which takes into account the fact that the elements of $\boldsymbol{\Delta}_i(t+1)$ might have different orders of magnitude.

The estimation problem amounts to solving $\min_{\omega,\boldsymbol{\theta}} f(\omega, \boldsymbol{\theta})$ under constraints that $\boldsymbol{\theta} \geq 0$, $\omega \in [0, 1]$, and that $S_i(t) \geq 0$ for all $t = 0, 1, \ldots, T$ and $i = 1, \ldots, K$. These latter constraints are guaranteed to hold if

$$\omega \geq \omega_{\min} \doteq \max_{i=1,\ldots,K} \max_{t=0,\ldots,T} \frac{I_i(t) + R_i(t) + D_i(t)}{\alpha_i \text{Pop}}.$$

We observe that, for fixed ω, the minimization of f with respect to $\boldsymbol{\theta} = (\boldsymbol{\beta}, \boldsymbol{\gamma}, \boldsymbol{\nu})$ can be done efficiently by solving a linearly constrained least-squares problem. We call this the inner step of the identification algorithm. The dependency of f on ω is instead non-convex, hence we approach this issue via an outer gridding on $\omega \in [\omega_{\min}, 1]$, as detailed in the following algorithm.

Algorithm 3.1 (Estimation of constant parameters):

1) Grid n values ω_i of ω in $[\omega_{\min}, 1]$. For each of these ω_i:
2) Solve the constrained least-squares problem $f_i^* = \min_{\boldsymbol{\theta} \geq 0} f(\omega_i; \boldsymbol{\theta})$ and let $\boldsymbol{\theta}_i^*$ be an optimal solution.
3) At the end of the loop, retain the ω_i value that yielded the minimal value of f_i^*, and return this ω_i along with the corresponding $\boldsymbol{\theta}_i^*$.

B. Model with time-varying parameters

While a constant-parameters model may be appropriate for describing a specific phase in the evolution of a pandemic, it can hardly capture its overall characteristics over an extended period of time. Clearly, the contagion rates $\beta_i(t)$ vary with changes in the behavior of the population, induced, for instance, by restrictive measures on people's mobility imposed by authorities. Similarly, the recovery and death rates $\gamma_i(t)$, $\nu_i(t)$ may change due to medical response policies that improve as knowledge and understanding of the virus progresses.

To incorporate time-varying coefficients into a tractable model, we consider the following parameterized families of time functions for the parameters, for $j = 1, \ldots, K$:

$$\beta_j(t) = \sum_{i=1}^{n_1} \beta_{ij} b_{ij}(t) \tag{8}$$

$$\gamma_j(t) = \sum_{i=1}^{n_2} \gamma_{ij} g_{ij}(t) \tag{9}$$

$$\nu(t) = \sum_{i=1}^{n_3} \nu_{ij} m_{ij}(t), \tag{10}$$

where $b_{ij}(t)$, $g_{ij}(t)$, and $m_{ij}(t)$, are given basis functions, and n_1, n_2, n_3 are the basis expansion orders. For each age class $j = 1, \ldots, K$, we define vectors $\boldsymbol{\beta}_j \doteq (\beta_{1j}, \ldots, \beta_{n_1 j})$, $\boldsymbol{\gamma}_j \doteq (\gamma_{1j}, \ldots, \gamma_{n_2 j})$ and $\boldsymbol{\nu}_j \doteq (\nu_{1j}, \ldots, \nu_{n_3 j})$ and the overall compound parameter vectors $\boldsymbol{\beta} \doteq (\boldsymbol{\beta}_1, \ldots, \boldsymbol{\beta}_K)$, $\boldsymbol{\gamma} \doteq (\boldsymbol{\gamma}_1, \ldots, \boldsymbol{\gamma}_K)$, $\boldsymbol{\nu} \doteq (\boldsymbol{\nu}_1, \ldots, \boldsymbol{\nu}_K)$.

Several choices are possible for the basis functions, like piece-wise constant functions, polynomial and exponential

functions, logistic functions, or mixtures thereof. For example, a logistic profile describes a smooth transition from one value of the parameter to another value, around a certain time instant; a simple two-parameter logistic profile for $\beta_j(t)$ would then be:

$$\begin{aligned}\beta_j(t) &= \beta_{1j} b_{1j}(t) + \beta_{2j} b_{2j}(t) \\ &= \beta_{1j} \frac{\exp(-(t-t_\ell)/\tau)}{1+\exp(-(t-t_\ell)/\tau)} \\ &+ \beta_{2j} \frac{1}{1+\exp(-(t-t_\ell)/\tau)},\end{aligned} \tag{11}$$

where β_{1j} has the practical meaning of infection rate for class i in early stages on the infection (i.e., for $t \ll t_\ell$), β_{2j} has the meaning of asymptotic infection rate, t_ℓ is the time at which lockdown measures become effective, and τ tunes the rapidity of transition from the pre-lockdown rate to the post-lockdown rate. In this case, we are assuming that t_ℓ and τ are known and fixed in advance. When this is not the case, we can include in the basis *many* functions of the form (11), each with different and suitably gridded values of t_ℓ and τ.

The parameters of a time-varying model can be identified using a regression technique similar to the one presented in the previous section. However, this is out of the scope of this paper, where instead we are interested in exploiting the model with time-varying parameters in order to introduce control policies that can affect the pandemic evolution.

IV. Model identification on Tennessee data

In this section, we apply the proposed constant-parameter model to the COVID-19 data from the state of Tennessee. To the best of the authors' knowledge, this was the only state we found that provides open data with the required age information. The dataset is publicly available at `https://www.tn.gov/health/cedep/ncov/data/downloadable-datasets.html`. This dataset covers the period from July 27th to December 16th. The number of daily cases, deaths and recoveries are subdivided in nine age classes: 0-10 years, 11-20 years, 21-30 years, 31-40 years, 41-50 years, 51-60 years, 61-70 years, 71-80 years, and over 80 years. In addition to this dataset, we retrieved information on the age distribution of the overall Tennessee population from [15].

We consider the constant-parameter model described in Sec. III-A. We use the technique illustrated in Algorithm 3.1 to identify the parameters of the model describing the contagion evolution for the different age classes. Data from September 4th[1] to November 20th were used to fit the model. This corresponds to 75% of the available data, the remaining of the available data were used as test data to evaluate the quality of the model prediction. As described in Algorithm 3.1, we compute the objective cost $f(\omega, \boldsymbol{\theta})$ as a function of ω, in order to select the best value for parameter ω. For the training data considered in our experiment, the optimal value resulted to be $\omega = 1$. In Table I we list the optimal values of the model parameters $\boldsymbol{\beta}$, $\boldsymbol{\gamma}$ and $\boldsymbol{\nu}$ corresponding to $\omega = 1$. We can observe that the optimal value of the mortality rate parameter ν_i decreases as the age decreases and is equal to zero in the younger age classes. This is consistent with the data on the COVID-19 mortality rate by age in Fig. 1.

[1]On September 3rd the Tennessee Department of Health updated its definition of an active case significantly lowering the number of active cases on that day and moving forward [16]. Therefore, we decided to discard previously collected data in order to have a coherent count of the recoveries.

TABLE I

Optimal values of the model parameters $\boldsymbol{\beta}$, $\boldsymbol{\gamma}$ and $\boldsymbol{\nu}$.

Class	$\boldsymbol{\beta}$	$\boldsymbol{\gamma}$	$\boldsymbol{\nu}$
0-10 years	0.0441	0.0893	0
11-20 years	0.1064	0.0910	0
21-30 years	0.1604	0.0914	2.195×10^{-5}
31-40 years	0.1267	0.0899	6.233×10^{-5}
41-50 years	0.1292	0.0901	2.061×10^{-4}
51-60 years	0.1186	0.0892	8.176×10^{-4}
61-70 years	0.0965	0.0874	2.437×10^{-3}
71-80 years	0.0921	0.0840	6.658×10^{-3}
81+ years	0.1040	0.0740	1.605×10^{-2}

TABLE II

Per-class cumulative number of deaths.

Class	No restriction	Selective lockdown	Uniform lockdown
0-10 years	6	6	6
11-20 years	2	2	2
21-30 years	97	77	43
31-40 years	240	186	101
41-50 years	748	571	288
51-60 years	2713	2026	940
61-70 years	6111	4503	2028
71-80 years	10279	3653	3326
81+ years	13069	4618	4195
Total	33265	15642	10929

After having identified the parameters of the model, we are now interested in projecting the estimated model forward in time in order to predict the future evolution of the contagion. To construct forward predictions, we use the multi-simulation prediction method described in [17] (Sec. 4.2). Fig. 2 shows the resulting per-class prediction. We can observe that the predictions nicely fit the real data for all the age classes. The data considered in this experiment describe the early stage of contagion, instead the predictions are constructed over a period five times longer than the one described by the data, covering all the contagion evolution until the end of the epidemic.

V. Contagion control by focused restrictions

In this section, we are interested in analyzing the effects on the contagion evolution of focused restrictions that act only on specific age groups. We thus have to consider a model with time-varying parameters, as described in Sec. III-B. In particular, we consider time-varying contagion rates $\beta_i(t)$. In order to simulate the effect of lockdown policies applied only to selected age groups, we impose that the parameters $\beta_i(t)$ corresponding to the two oldest classes have a two-parameter logistic profile as described in Eq. (11). For both classes, we set the parameter β_{1j} equal to the corresponding optimal value of the constant-parameter model described in the previous section and β_{2j} equal to zero. All the other parameters of the model, including the contagion rates $\beta_i(t)$ corresponding to the other age classes,

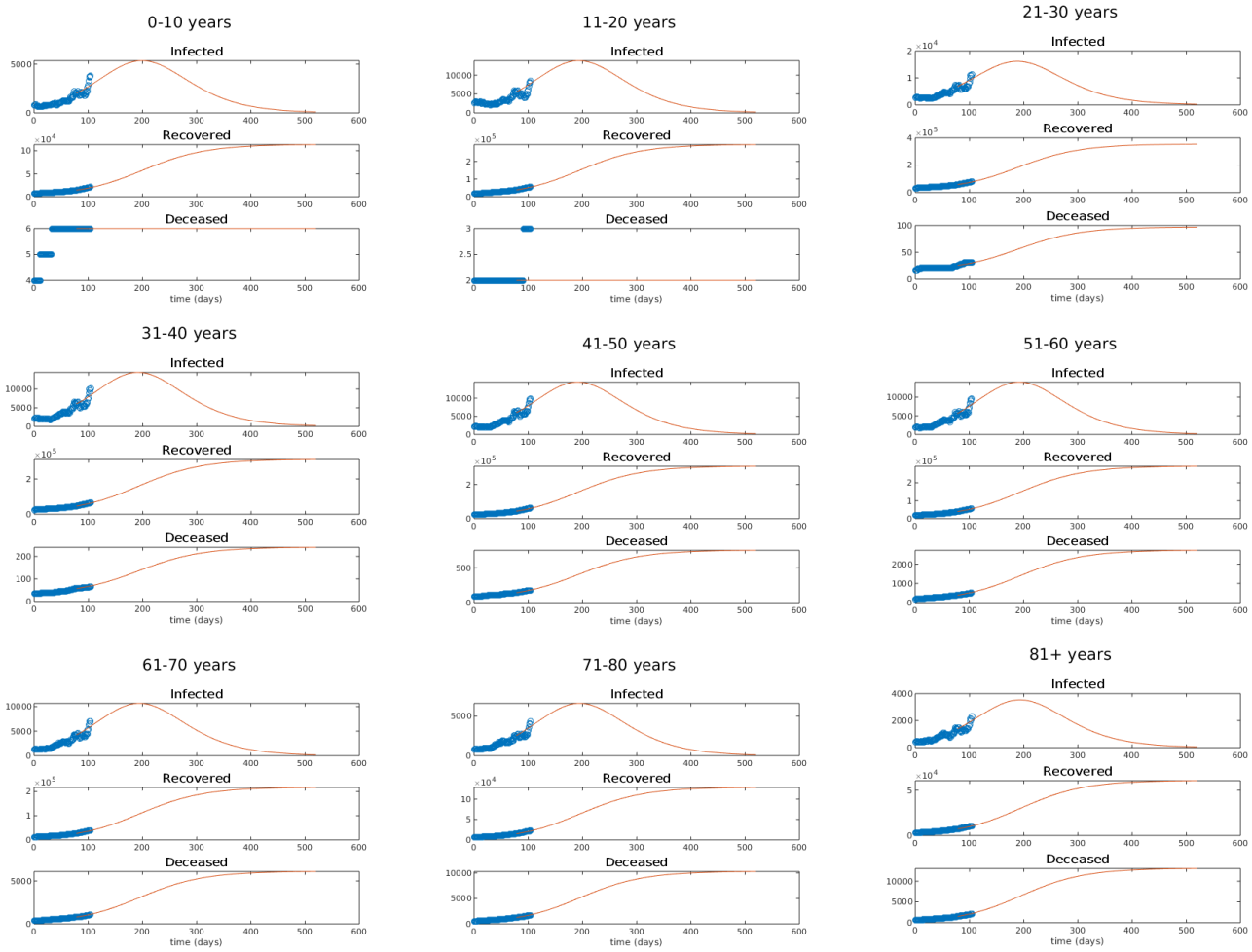

Fig. 2. Per-class multi-simulation prediction with the constant-parameter model. The red curve describes the multi-simulation prediction, and the blue circles represent the actual data use for model training.

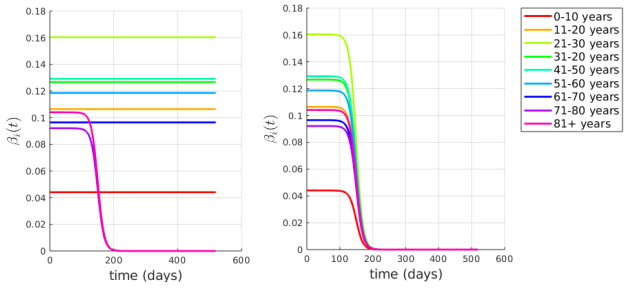

Fig. 3. Time-varying contagion rates $\beta_i(t)$ as function of time. Selective lockdown (left), uniform lockdown (right).

are considered constant and their values are set equal to the optimal values of the constant-parameter model. Fig. 3 (left) shows the resulting parameters $\beta_i(t)$ as function of time, where we set $t_l = 150$ and $\tau = 10$ for the two oldest age classes. In order to evaluate the effects of such type of restrictions, we compared this scenario against other two cases: the first one considers a uniform lockdown applied to the entire population, instead the second one considers the case where no restrictions are applied. The case of a uniform lockdown is simulated by imposing that all the contagion rates $\beta_i(t)$ have a two-parameter logistic profile, where β_{1j} and β_{2j} are defined as previously described. Fig. 3 (right) shows the shapes of the parameters $\beta_i(t)$ in this scenario. The case without restrictions is simulated by considering the constant-parameter model identified in the previous section. We now use the multi-simulation technique described in [17] to project forward in time these three scenarios. Fig. 4 depicts the resulting multi-simulation predictions. We can observe that in the case of a selective lockdown, even though the restrictions are applied only to the two oldest classes, the effects are visible in all the age classes, significantly reducing the spread of the contagion. Moreover, in Table II we compare the cumulative number of deaths in the three scenarios. In particular, it is important to observe that a selective lockdown applied only to the two oldest age groups can result in a significant reduction of the total number of deaths, approximately halving it. In addition, the results in Table II show that a uniform lockdown, which has a much stronger socio-economic impact, provides only a slight reduction in the number of total deaths as compared to a selective lockdown applied only to the two oldest age groups.

VI. Conclusions

In this paper we presented a modified SIRD model with age classes for the COVID-19 infection evolution. This model allows for introduction and analysis of control policies

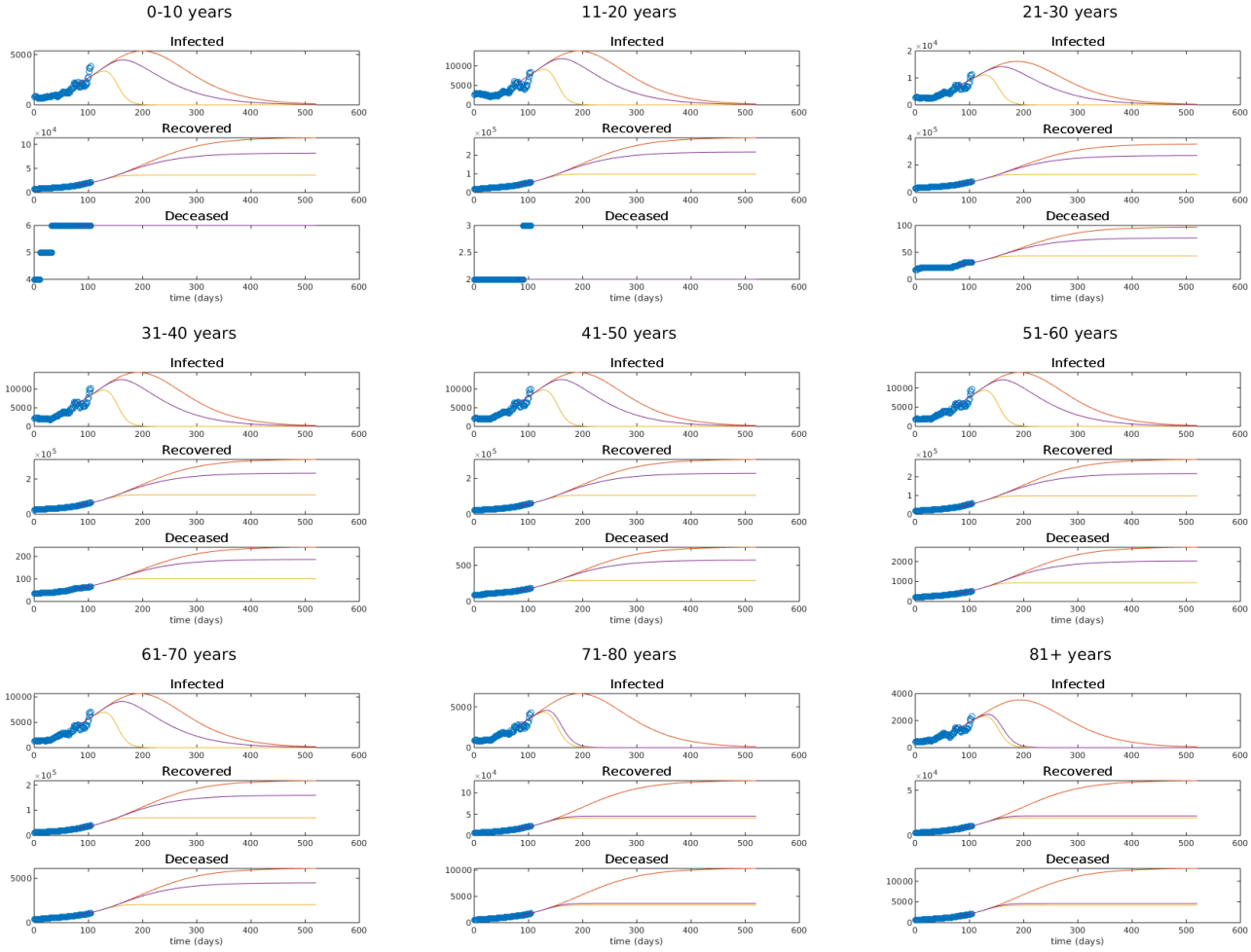

Fig. 4. Per-class multi-simulation prediction. The red curve corresponds to the case without restrictions, the purple line corresponds to the case of a selective lockdown, the yellow line corresponds to the case of a uniform lockdown, and the blue circles represent the actual data used for training.

based on age-selective lockdowns. In particular, we studied the effects of a selective lockdown applied only to the older classes of the population. The simulations suggest that such selective lockdowns may provide a reduction of the mortality rate similar to the one obtained with a uniform lockdown, while having a much lighter socio-economic impact.

REFERENCES

[1] World Health Organization, "Coronavirus disease (COVID-19) situation report," *https://covid19.who.int/*, 2020.

[2] Centers for Disease Control and Prevention, COVID-19 Response, "CDC Covid Data Tracker," *https://covid.cdc.gov/covid-data-tracker*, 2020.

[3] R. Chowdhury et. al., "Dynamic interventions to control COVID-19 pandemic: a multivariate prediction modelling study comparing 16 worldwide countries," *European Journal of Epidemiology*, vol. 35, no. 5, pp. 389–399, 2020.

[4] Kiesha Prem et.al., "The effect of control strategies to reduce social mixing on outcomes of the COVID-19 epidemic in Wuhan, China: a modelling study," *The Lancet Public Health*, 2020.

[5] Mariam Claeson and Stefan Hanson, "COVID-19 and the swedish enigma," *Lancet (London, England)*, 2020.

[6] Jennifer Beam Down et. al., "Demographic science aids in understanding the spread and fatality rates of COVID-19," *Proceedings of the National Academy of Sciences*, vol. 117, no. 18, pp. 9696–9698, 2020.

[7] Kai Liu, Ying Chen, Ruzheng Lin, and Kunyuan Han, "Clinical features of COVID-19 in elderly patients: A comparison with young and middle-aged patients," *Journal of Infection*, 2020.

[8] Clara Bonanad et. al., "The effect of age on mortality in patients with COVID-19: a metanalysis with 611,583 subjects," *Journal of the American Medical Directors Association*, 2020.

[9] Graziano Onder, Giovanni Rezza, and Silvio Brusaferro, "Case-fatality rate and characteristics of patients dying in relation to COVID-19 in italy," *Jama*, vol. 323, no. 18, pp. 1775–1776, 2020.

[10] Fei Zhou et. al., "Clinical course and risk factors for mortality of adult inpatients with COVID-19 in Wuhan, China: a retrospective cohort study," *The Lancet*, 2020.

[11] Ryosuke Omori, Ryota Matsuyama, and Yukihiko Nakata, "The age distribution of mortality from novel coronavirus disease (COVID-19) suggests no large difference of susceptibility by age," *Scientific Reports*, vol. 10, 2020.

[12] et. at. Marilia R. Nepomuceno, "Besides population age structure, health and other demographic factors can contribute to understanding the COVID-19 burden," *PNAS*, vol. 117, no. 25, pp. 13881–13883, 2020.

[13] Martin Kulldorff, Sunetra Gupta, and Jay Bhattacharya, "The Great Barrington Declaration," *https://gbdeclaration.org/*, 2020.

[14] Tennessee State Government, "Tennessee COVID-19 Unified Command Dashboard," *https://www.tn.gov/governor/covid-19/statewide-data.html*, 2020.

[15] U.S. Census Bureau, "Sex by age american community survey 1-year estimates," *https://censusreporter.org*, 2019.

[16] Tennessee Department of Health, "COVID-19 critical indicators," *https://www.tn.gov/content/dam/tn/health/documents/cedep/novel-coronavirus/CriticalIndicatorReport.pdf*, 2020.

[17] Giuseppe C. Calafiore, Carlo Novara, and Corrado Possieri, "A time-varying SIRD model for the COVID-19 contagion in Italy," *Annual Reviews in Control*, 2020.